Ultra low wind resistance enclosure for a 100 m telescope

Thomas D. Ditto*[a] and Joseph M. Ritter[b]
[a]DeWitt Brothers Tool Co., Inc., Ancramdale, NY, USA 12503-0010
[b]Institute for Astronomy, Univ. of Hawaii, 34 Ohia Ku Street, Pukalani, HI USA 96768-8288

ABSTRACT

We discuss a transmission primary objective grating (POG) telescope that is nearly flat to the ground with its secondary components buried below ground in a protected environment that enjoys a controlled atmosphere. Temperature gradients can be held steady by sealing this enclosure. End-to-end ray paths need not be interrupted by spiders or other structural support elements. Unlike mirror and lens telescopes, this layout is intrinsically off-axis. Light diffracted from a POG at a grazing angle can be collected a few meters below the POG, and the substructures do not require a deep excavation, as would be required for buried on-axis mirrors such as a zenith tube. The POG principle can take advantage of the rotation of the earth to acquire spectra sequentially, so active tilt and rotate axes are not necessary during observations. The POG aperture is extensible as a ribbon optic to kilometer scale at a linear increase in cost, as compared to other choices where infrastructure grows as the cube of the telescope size. The principle of operation was proven in miniature during bench tests that show high resolution spectra can be obtained at angular resolutions equal to seeing. Mathematical models of the underlying relationships show that flux collection increases with increased angles of grazing exodus even as efficiency decreases. Zemax models show a 30° field-of-view and the capacity to take spectra of all sources within that very wide field-of-view. The method lends itself to large apertures, because it is tolerant of POG surface unevenness.

Keywords: enclosure, wind, turbulence, primary objective, grating, holography

1. INTRODUCTION

Nothing better symbolizes astronomical telescopes than their unique enclosures that can pirouette to track the night sky. In recent years when giant telescopes were being readied for development, the scale of their proposed infrastructure grew as the cube of the telescope diameter, and the cost of shelter began to outpace the astronomical instruments these enclosures were supposed to house. Moreover, the profile of the enclosure presents a wind break. Computer and wind tunnel models suggest that when the roof was open, the interior air pressure would both resonate and exhibit complex temperature gradients. Given that the buildings were for use on mountain tops or high plateaus where weather extremes are commonplace, it became difficult to imagine any enclosure other than a hangar to protect the telescope during its down times. The giant 100 m OWL was expected to operate in the open air during observations. If ambitious plans for giant telescopes have been scaled back of late, it is due, in part, to the complications posed by their enclosures.

The zenith tube is a type of telescope that does not track the sky, and it is conceivable that its static pose would overcome many of the structural issues associated with giant telescope. A zenith tube could be simply buried below the ground, and its roof could be near to ground level. This would be a difficult roof to construct for a 100 m scale telescope, but there are some stadiums with roof designs that open up to the sky. Needless to say, the excavation would be deep and expensive on rocky mountain tops, but we have dynamite. A more serious problem is with the zenith tube itself. It cannot alter its declination, so only the seasonal variations in the earth's tilt would offer new sections of sky. While it is true that time domain integration sensors have revolutionized the integration period of a zenith tube, and the secondaries and tertiaries of parabolic primaries have been demonstrated to improve field-of-view (FoV), the zenith tube cannot track the precession of a star for more than a few hundred seconds in equatorial zones.

Our novel design for a telescope, introduced in 2002 as the "Dittoscope," uses a primary objective grating (POG) configured to collect at a grazing exodus angle.[1] It can alter its declination, although it works conveniently over the Great Circle. That said, the scale of the primary along the diffraction axis is extensible, and kilometer scale apertures in one dimension can be contemplated. More to the point of the present inquiry, the optical path is intrinsically off-axis, allowing for a ray path that travels sideways from the primary to the secondary. This feature results in an enclosure that can be held flat to the ground presenting virtually no wind profile.

* 3d@taconic.net; phone +1 518 329-1275; fax 1 518 329-7743; home.earthlink.net/~scan3d

2. POG PRINCIPLES

In the nineteenth century a type of slitless spectroscopy was developed using a coarse diffraction grating placed in front of a conventional telescope. The resulting spectrograms were noisy at best, and the overlap of adjacent objects resulted in ambiguous spectra. The pointing of a the slitless POG was no different than an ordinary telescope when the grating was a transmission type, but when a reflection grating was used, the telescope had to point down to see up. This presages a novel configuration we proposed in 2002 nearly a century after the original slitless POG lost favor. Ours has a slit. [2-5]

When the POG has a pitch equal to the wave length of the radiation at its zenith, it will reconstruct its first-order for that wave length at angle of 90°. Of all types of gratings, these very high frequency gratings have the widest free spectral range, that is, the first-order has wavelengths where higher-orders do not overlap. Since these waves are collected near the edge of the grating, the geometry lends itself to flat telescope. The grating length can be many times greater than the secondary mirror that collects the dispersion from the grating. The geometry is shown in Figure 1.

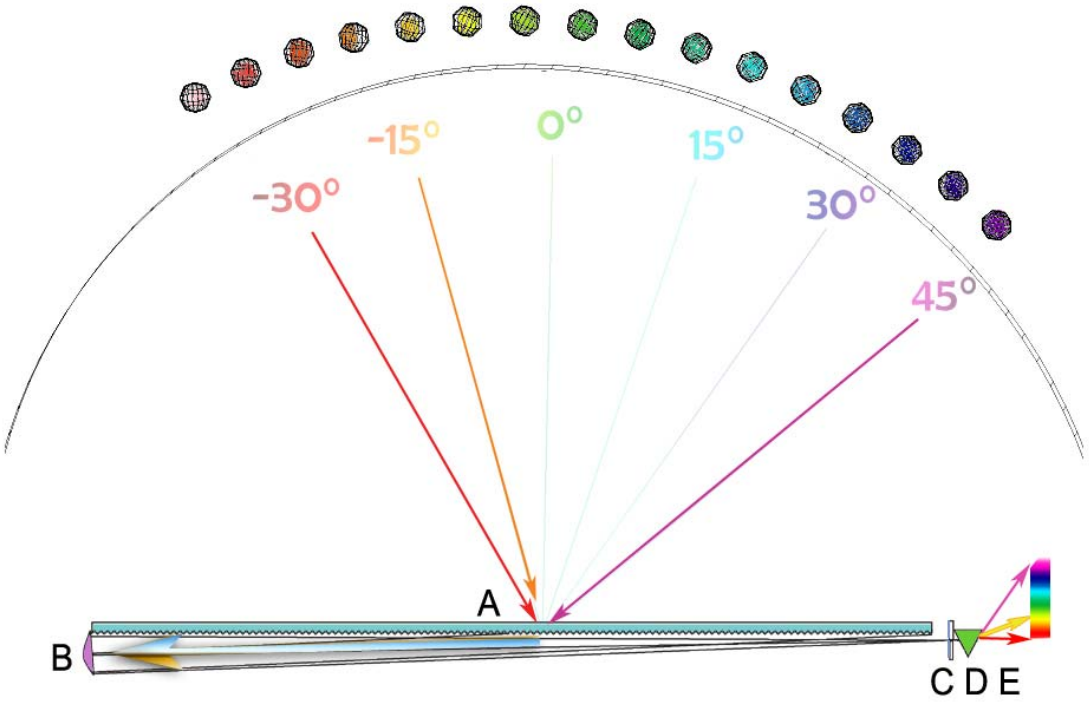

Fig. 1 POG **A** redirects light to secondary parabolic mirror **B** that focuses light on slit **C** of spectrograph **CDE**.

While it is true that such geometric optics belie the difficulty of making the physical optics workable, we have addressed some of these issues in other disclosures. If the reader will allow that such architecture can be made to work, there is a marked difference in the paradigm of physical plant needed when compared to traditional telescopes.

2.1 Sizing the primary

The maximum length of the POG L is determined by the receiving angle r and the diameter of the secondary mirror D, Figure 2. The dependency is $L = D/\cos(r)$.

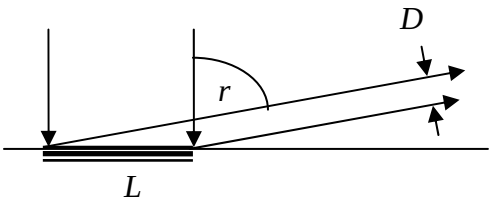

Fig. 2 POG length L

In the Graph A of Figure 3, grating lengths up to a kilometer are plotted against mirror diameters. Receiving angles are separately plotted in five cases from 85° to 89° in 1° steps. The ratio of L:D is the anamorphic magnification of the POG and is plotted in Graph B on a log scale for r between 85° and 89.4°.

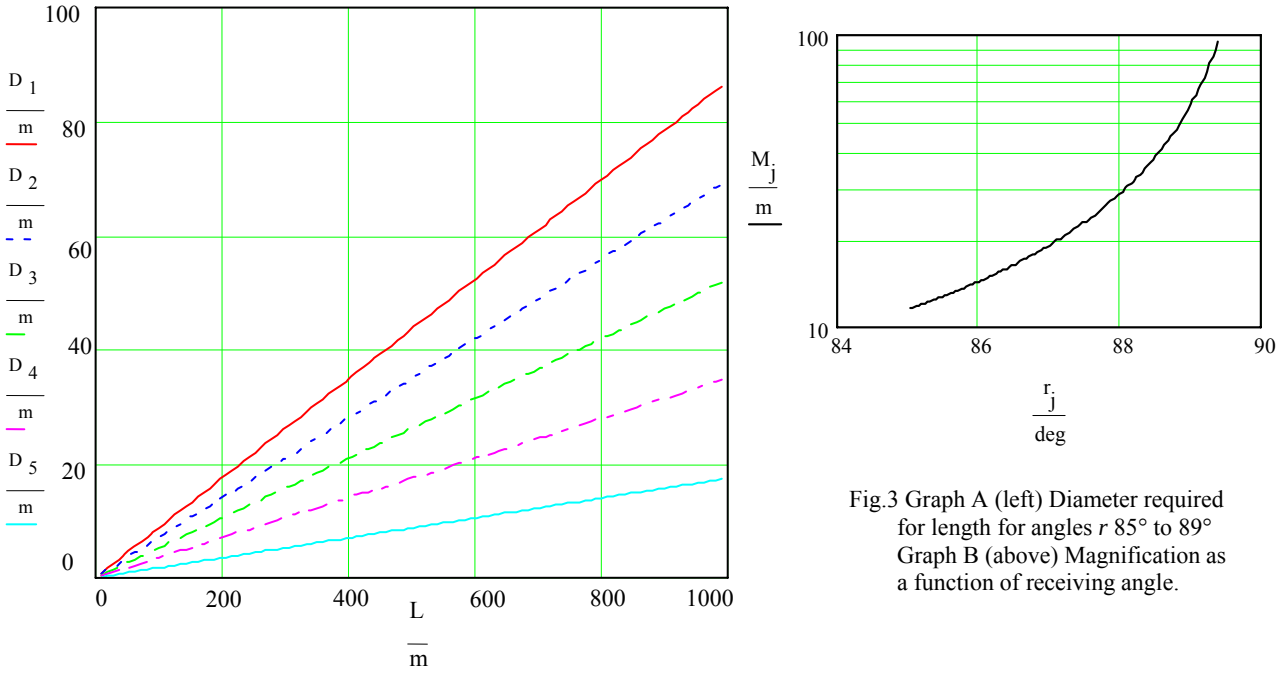

Fig.3 Graph A (left) Diameter required for length for angles *r* 85° to 89° Graph B (above) Magnification as a function of receiving angle.

It is interesting to consider that the secondary mirror sizes graphed in Figure 3 begin to approach the scale of primary mirrors recently contemplated for future giant telescopes. For example, a 50 m secondary will permit a kilometer scale POG at 87° grazing exodus. This POG is a gigantic primary objective that could approach 50,000 m^2 of collection area.

2.2 Segmentation and declination

When the POG is a plane grating it can be segmented into rectangular facets. This affords an opportunity to put up baffles to contain the free spectral range by masking competing higher-orders. Alignment of facets could be done under guidance of laser interferometry. The mechanicals might involve piezo electric pistons.

If the POG is strictly aligned with the planet's rotation, that is, along lines of longitude, the telescope can be operated in a static pose like a zenith tube. However, unlike a zenith tube, the latitude it will see can be adjusted during daylight by changing its angle of declination along the axis of diffraction.

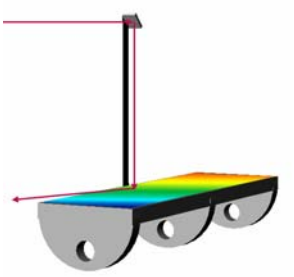

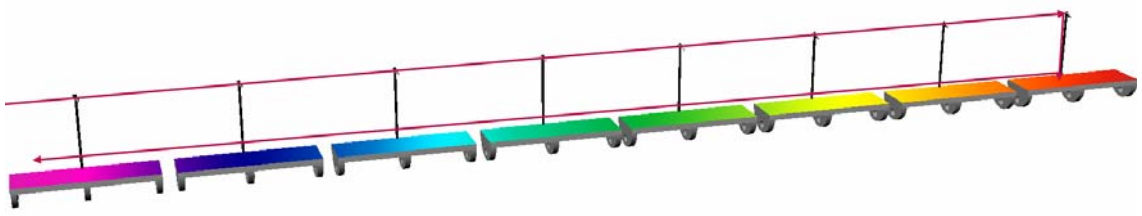

Fig. 4 Discrete reflection POG modules with ganged laser interferometric alignment masts

In the past, the construction of telescopes from monolithic components resulted in the concept of "first light," the moment when enough of the requisite parts of a telescope were in place and used for the first time. Without near-completion of all the components: the mirror, its superstructure, and the enclosure; it was impossible to begin observations and shake down the instrument. A POG telescope will begin to function with its first facet in place. For this reason, an extensible instrument can be built piecemeal as a test bed, and if it demonstrates feasibility, the same site could ultimately host larger versions of the same telescope.

3. POG MODEL

3.1 Grating behavior

To bury the secondary completely below ground, the POG must be a transmission type. For most terrestrial wavelengths the glass will pass those wavelengths that also penetrate the atmosphere. One Zemax model supposes a 5 cm glass plate as the plane diffraction grating blank. The grating rules are on the bottom of the plate. For this model, discussed below, we chose a grating pitch of 1.805 lines/μm or 554.017 nm. This resulted in the POG collecting 550 nm from the zenith. Our outside wavelengths were 398.94 nm that diffracted at 15.823° off the normal and 0.701055 nm that diffracted at -15.822° off the normal. These are well within the free spectral range, Figure 5.

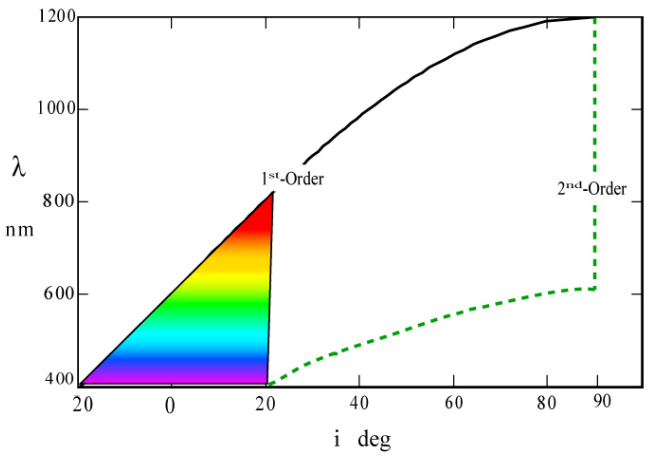

Fig. 5 Free spectral range for 1800 line/mm plane grating

If the model is for a 100 m POG, a secondary parabolic mirror of 10 m at a grazing angle of 82.8° will be in the ray path of the diffracted light. Zemax does not predict efficiency, but we know from related work with PCGrate® models near grazing incidence that efficiency will be limited to about 25%, although one of the polarization axes will be 50% or more when the grating is holographic and has a sinusoidal blaze. The light gathering of the a 100 m POG collecting over 1000 m^2 will be about the same as a 250 m^2 primary objective mirror.

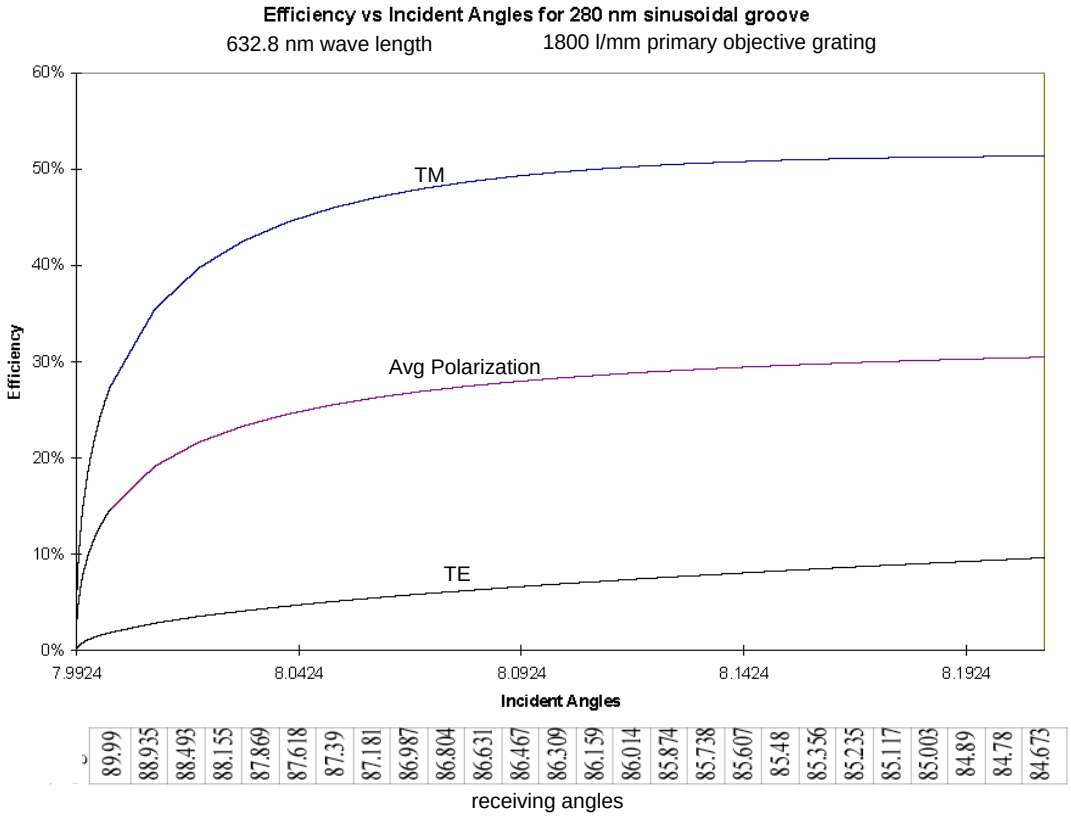

Fig. 6 PCGrate® prediction of the HeNe line near grazing exodus for a 555.5 nm POG

3.2 Zemax model

As with any telescope design, there are an enormous number of variations possible due to the many parameters involved. We began our investigation by looking at the transmission POG, giving it a 100 m x 10 m rectangular shape. Then we chose an F/5 10 m circular secondary to focus on a slit. The focal length of the secondary mirror is not constrained by the mechanical motion problem of housing or moving it, since it is static and positioned at the periphery of a 100 m primary. This allows for the choice of a narrow FoV in the lateral dimension where the image is focused exclusively by reflection optics. We have chosen to investigate very large secondary spectrograph gratings, because the high resolution of the primary can be exploited when the secondary grating matches POG performance. A preliminary ray trace of the design appears as Figure 7.

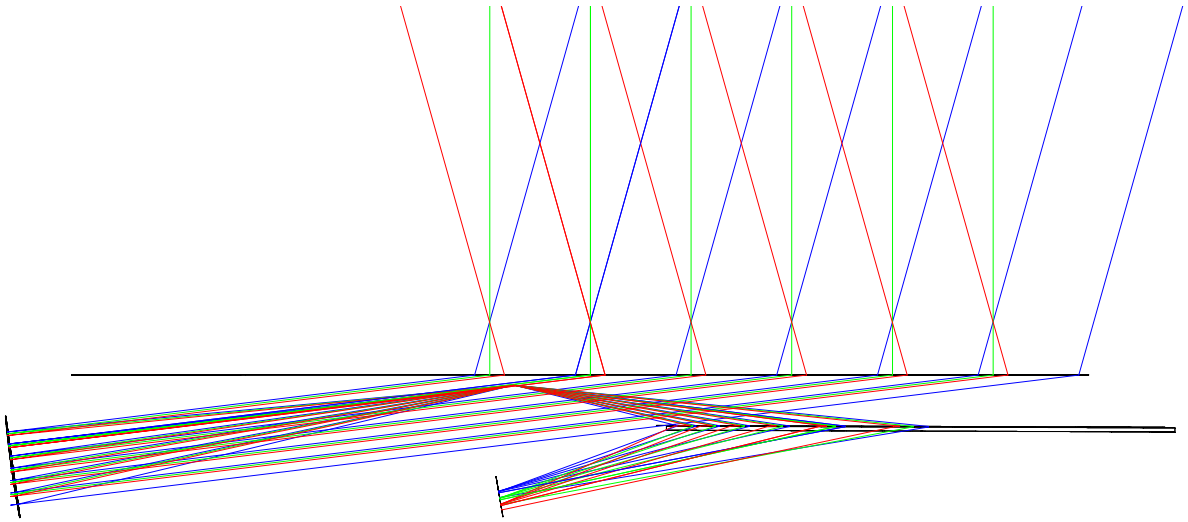

Fig. 7 Ray tracing in Zemax for transmission POG above with mirror secondary on left and spectrometer on right, below.

Interesting features of the model include the use of a folding mirror just below the POG to redirect the light to the spectrograph. This feature keeps all of the useful light inside a subterranean shelter. The folding mirror also could serve as the slit, since its width will restrict the wavelengths available to the spectrograph. For a 100 m telescope, the slit would be 1 cm or less, Figure 8.

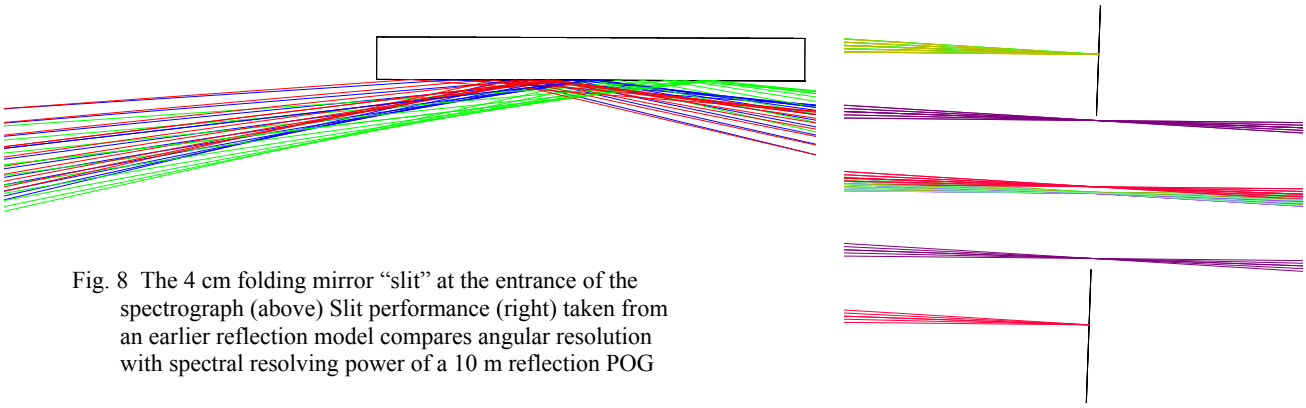

Fig. 8 The 4 cm folding mirror "slit" at the entrance of the spectrograph (above) Slit performance (right) taken from an earlier reflection model compares angular resolution with spectral resolving power of a 10 m reflection POG

In an earlier Zemax model made for a 10 m reflection POG we have shown that a 300 μm slit will provide masking that will block off-axis rays. At 550 nm, the wavelength can be resolved to 0.005 Å over an angular resolution is 0.36 arc seconds. Increases in bandwidth are proportional to slit width with a corresponding decrease in angular resolution.

Very high spectral resolving power may have utility in radial velocity measurements as used in exo-planet surveys. The POG telescope is a multiple object spectrometer. Every source has its spectrum taken in the course of a night. For this

reason, we have studied large secondary spectrograph gratings. A holographic grating in the present design uses two chirped high frequency gratings that are superimposed inversely on either side of a glass plate as detailed in Figure 9.

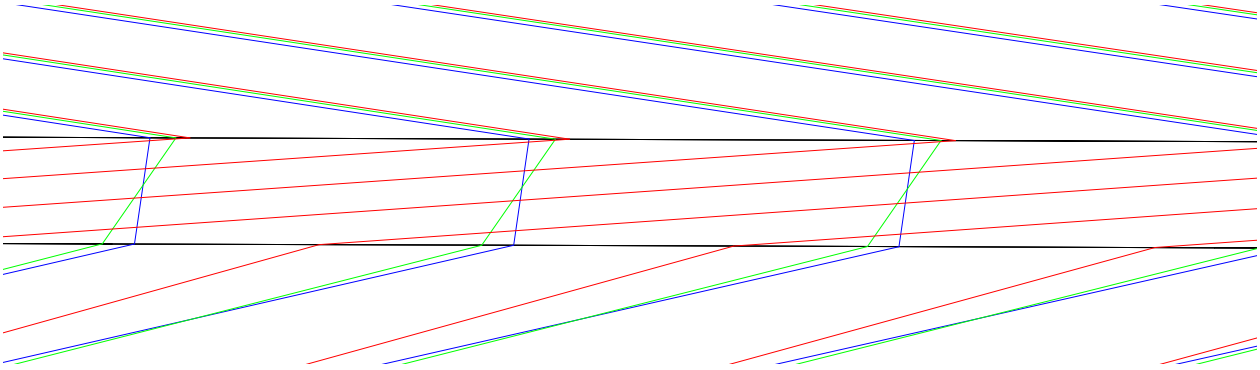

Fig. 9 Dual chirped frequency holographic grating uses both sides of the plate to focus the spectrum over workable range.

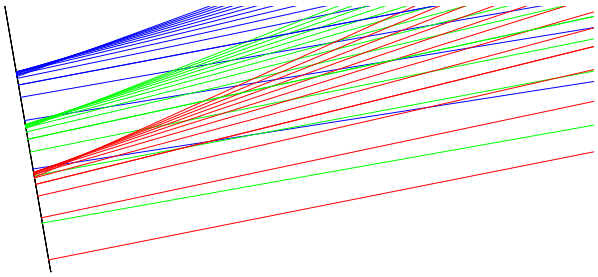

Fig. 10 Focal plane of spectrograph as of publication date

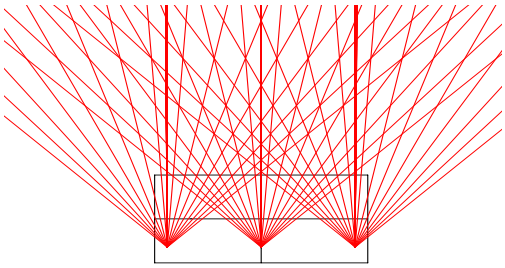

Fig. 11 Lateral displacement at the focal plane

A single hologram by itself at these near wavelength variable pitch spacings broadly separates the spectra, as does the POG, but a nearly inverse sequence of pitches brings the original back as a narrowly spaced spectrum that can be collected over a reasonably scaled focal plane. As of the date this publication the concept is being studied. It does not yet focus sharply over its entire 50 m length (Figure 10) and presents efficiency issues due to the double pass. However, holographic fabrication is an attractive option for large gratings and the only practical process of generating the non-linear modulation.

The lateral focus of the POG telescope is effectively the same as a conventional telescope. In Figure 11 we show objects on the focal plane that are separated in the sky by 18 arc seconds north to south at a single wave length. Magnification in the lateral non-diffracted is determined by the primary objective. The extremely anamorphic magnification of the POG leads to endemic astigmatism that must be corrected. There are surfaces between the parabolic mirror and the focal plane that provide for an opportunity to make the correction. Further study is needed to determine if astigmatism is wavelength dependent. If so, its correction may involve additional diffraction optics.

3.3 Ground site

Building an ultra low wind resistant enclosure of a 100 m POG telescope is largely a matter of excavation rather than elevation. The POG lends itself to a trough excavation which is long relative to its width. The trough must be at least as deep as a secondary mirror at both ends. There will be symmetrical mirrors on both sides of the enclosure to acquire the sky in inverse order of spectral lines. The redundancy will play a role in calibrating the temporal spectrograms that are assembled during data reduction, as well as doubling the flux collected during an observation cycle.

A cross sectional rendering of the installation appears in Figure 12. The POG is a ribbon of glass, although it may be made of segments. Just below it is a small folding mirror. Large secondary parabolic mirrors appear on either side. They are immobile save for fine adjustments. The spectrograph gratings, on the other hand, pivot on their long axis to parallel

the POG which pivots to a designated line of right ascension during the day, but can be locked down during observations at night. Spectrograph cameras are shown in blue and are positioned at the deepest part of the assembly.

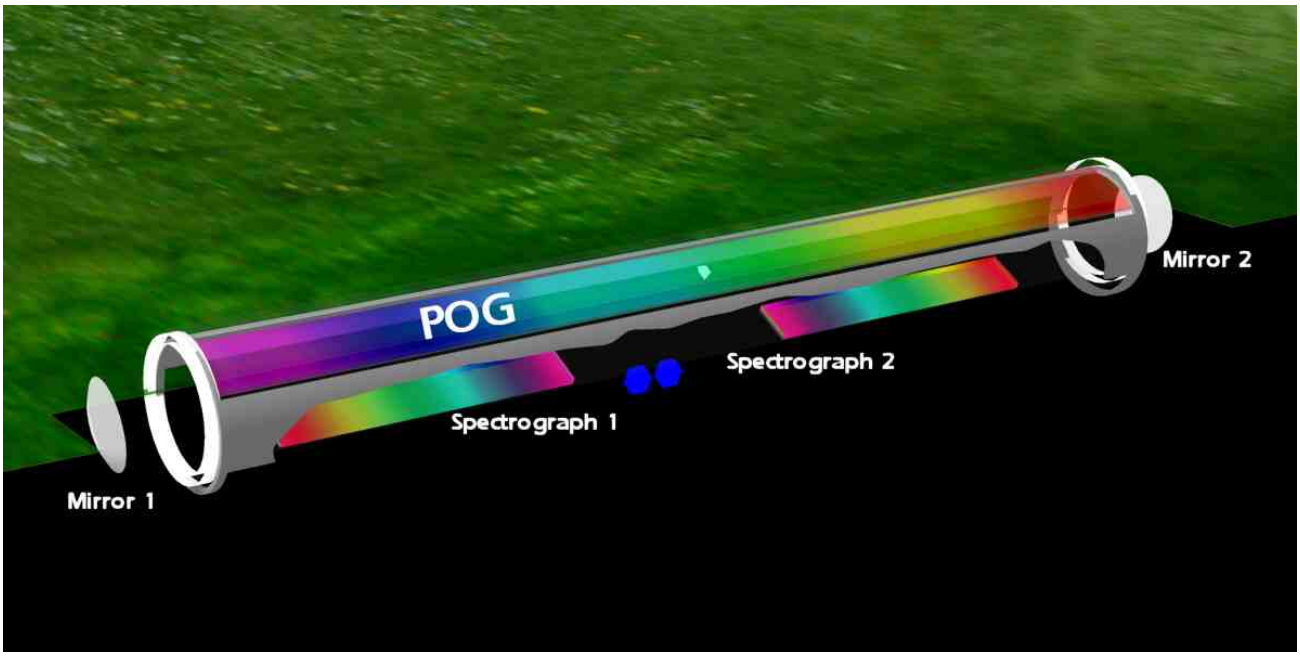

Fig. 12 Cross section of a terrestrial POG telescope scaleable to kilometer aperture along the axis of diffraction

As viewed from above without the cutaway of Figure 12, the POG telescope might look like this:

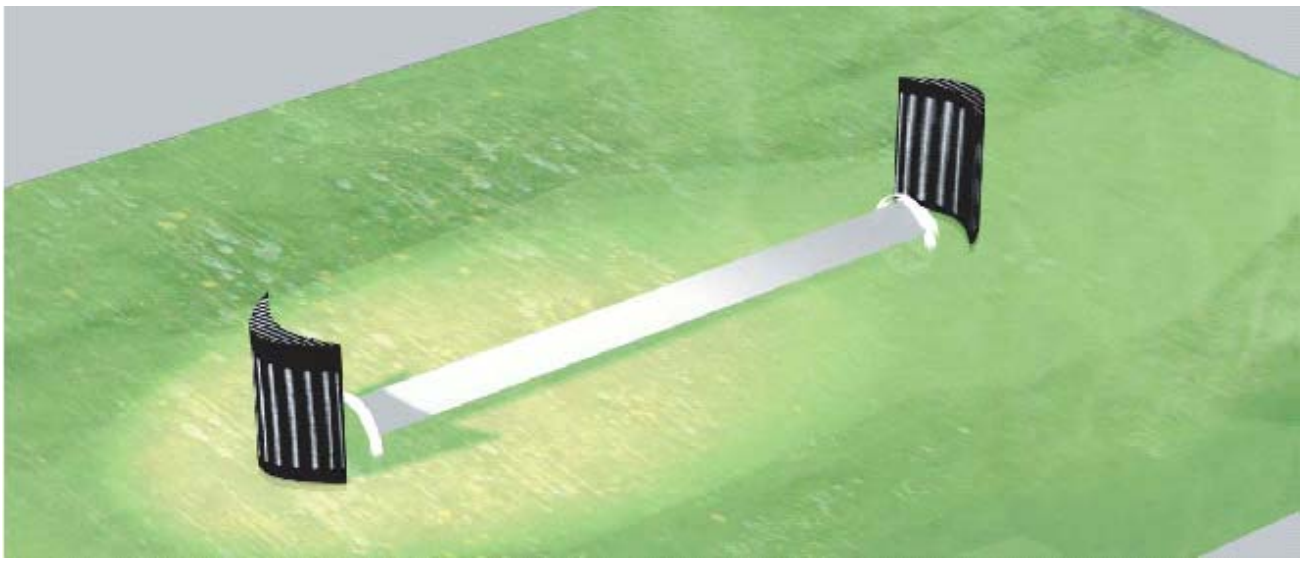

Fig. 13 A ground level POG with its daytime cover. Armatures rotate it to a chosen declination for the night. Two black towers used as windbreaks are constructed with internal baffles.

4. OBSTACLES

There has never been any serious question that the first principles upon which the POG telescope rests are sound. A simple bench demonstration made with a 50 mm POG, a camera lens, and a fiber fed spectrometer showed conclusively that the angle of incidence upon a grating could be correlated with the acquired wavelength. An example of the output is shown in Figure 14.

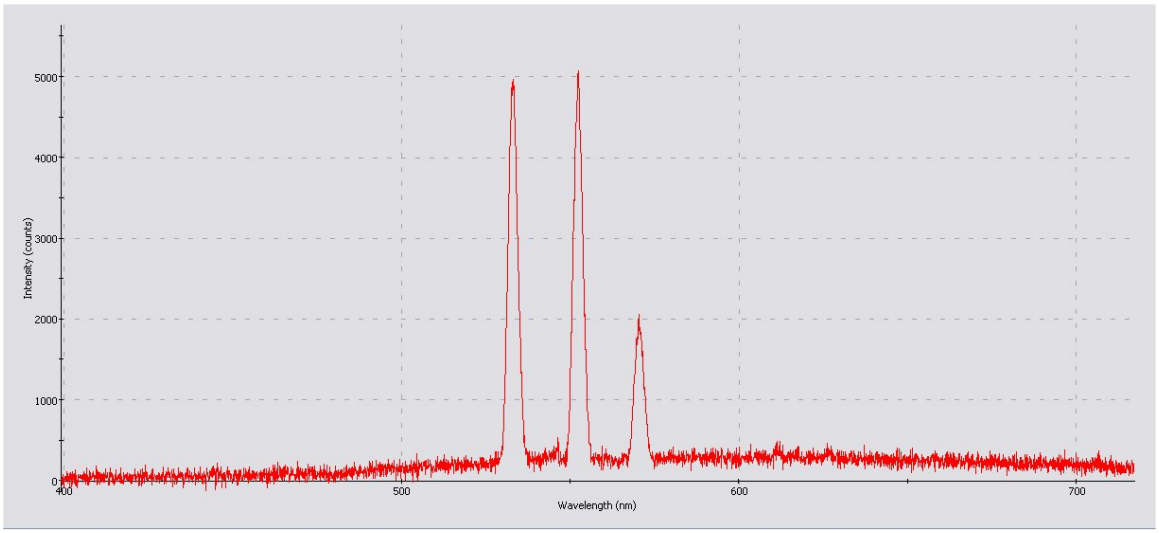

Fig. 14 Bench top demonstration: Output from a secondary spectrometer for three sources spaced apart by a few degrees.

First principles notwithstanding, some caveats have been raised with regard to the principle being used for astronomy. The list includes questions about flatness tolerances, flux collection, and a corollary, integration time. We are investigating these possible show stoppers. There might be a fatal flaw.

4.1 Flatness tolerance

Perhaps because the figure of a mirror limits its performance, there was a concern that it would be impossible to maintain a workable grating flatness over excursions of 100 m. This is not as serious a problem in diffraction as it is in reflection telescopes. It can be shown that the theoretical limit of resolution of a grating can be achieved by a grating that is flat to the wavelength that it is resolved. Over a long excursion where the theoretical resolution is extremely high, a diffraction grating is very forgiving with regard to its flatness.

However, there is a problem with phase tolerance, especially at grazing exodus. A flat grating with imperfect groove spacing will exhibit significant aberration. These tolerance criteria must be determined. What can be said in the context of the enclosure study is that certain environmental controls can be put in place to hold a given grating to a precise temperature because of its convenient access to the thermally controlled environment below it.

4.2 Flux collection

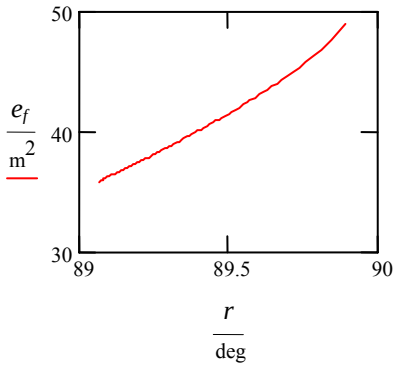

Fig. 15 Effective efficiency increases even as receiving angle approaches 90°.

At specific angles over narrow wavelengths diffraction gratings can be extremely efficient, but efficiency decreases when the incident angles are broad, the wavelengths run a wide gamut, and the receiving angle approaches grazing. We can show that as the receiving angle increases toward grazing, the concomitant extension of the POG length increases more quickly than the losses from lowered efficiency. If the effective efficiency is taken as the product of the efficiency curve of Figure 6 with growth in collection area derived from the increase in length of Graph B of Figure 3, we see a net increase in flux collection shown in the graph of Figure 15. This benefit appears even at very high angles of grazing exodus.

That said, gratings with optimal performance present fabrication issues. A sinusoidal groove that falls out naturally from holographic fabrication does not have a preferential blaze for one reconstruction angle or another. Only its depth can be controlled. Yet holography is probably the most likely means of fabrication. In all likelihood, a POG will be a surface relief grating, but volume types with restricted angles of incidence and reconstruction with favored wavelengths will be more efficient. The design may be subject to a specialty requirement in astronomy such as acquiring a bio-marker band at a very precise location. An embodiment of a POG with a high efficiency grating may be a choice for some special assignment of this type.

4.3 Integration time

With a static POG in the strict east/west orientation, collection is controlled by the rate of precession. For precession along the Great Circle the transit rate is 15 arcseconds of angle per second of time. At 550 nm, a wavelength can be resolved to 0.005 Å over an angular resolution is 0.36 arc seconds. Increases in bandwidth are proportional to slit width with a corresponding decrease in angular resolution. The instrument will be light starved when operating at its maximum angular resolution due to short integration times.

The Grating Equation can be written as:

$$\lambda = \frac{(\sin(i) + \sin(r))}{n} p \tag{1}$$

where:
λ = wavelength of radiation
i = incident angle
r = receiving angle
p = grating period
n = diffraction order

If the meridian is tagged as time t = 0, the angle of incidence i upon the POG can be calculated as $i = \omega t$. Solving for t in the Grating Equation we have:

$$t = \frac{a\sin\left[\frac{(n\lambda - p\sin(r))}{p}\right]}{\omega} \tag{2}$$

The integration time can then be known from Equation (3) by bracketing λ in Equation (2) for a wavelength band λ_b.

$$t_b = \frac{\arcsin\left[\frac{n[\lambda_b + \lambda] - p\sin(r)}{p}\right]}{\omega} - \frac{\arcsin\left[\frac{n\lambda - p\sin(r)}{p}\right]}{\omega} \tag{3}$$

If the bandwidth is restricted to one discrete wavelength, the integration time is zero. The telescope only produces spectra for sources in precession. In an example graphed in Fig. 16, integration times for wavelength bands from 0 to 1 Å width λ_b are the nearly same for reconstruction angles r = 85° and r = 89°. The calculation confirms our earlier published assertion that the worst case integration time for the POG telescope on earth is 2.3 sec per Å.[1]

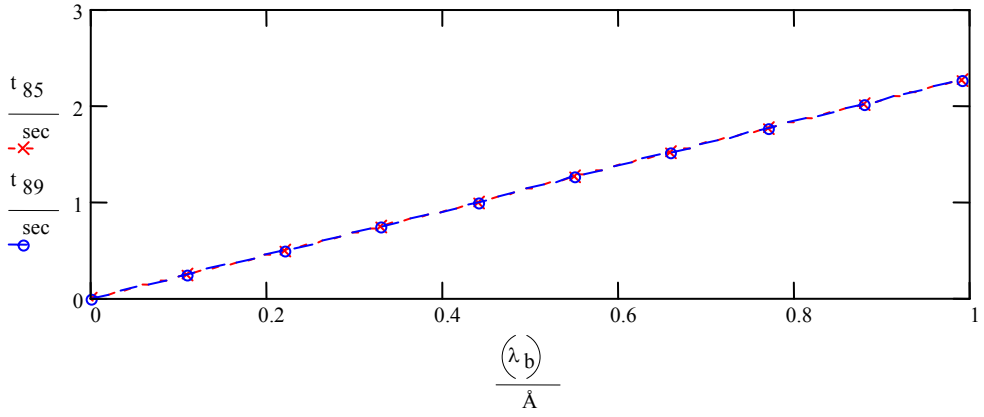

Fig. 16 Integration times for bandwidths $\lambda_b < 1$ Å for $r = 85°$ and $r = 89°$

A similar problem affects zenith tubes that record with photographic plates, but the introduction of the time domain integration CCD permitted integration time to be extended over the entire transit period within the telescope's FoV.

Taking instruction from that solution, it is possible use multiple slits to extend the effective integration time to the transit period over the secondary mirror's FoV. This dependency makes the integration time a slave to the secondary mirror's FoV. Redefining the receiving angle *r* as the grazing angle θ where (90° – *r*) = θ we can write the Grating Equation as

$$\cos(\theta) = \cos(\theta_0) - \sin(\omega t) \tag{4}$$

$$\text{where } \cos(\theta_0) = n\frac{\lambda}{p}$$

To obtain the effective integration time tef when the POG is viewed by a secondary mirror with a field-of-view Θ we use Equation (4) and set θ_0 to 90° where λ starts at 0. This gives us the complete arc of the sky as received by the secondary. Solving Equation (4) for t_{ef} we have

$$t_{ef} = \frac{\arcsin(\cos(\theta_0) - \cos(\theta_0 + \Theta)}{\omega} \tag{5}$$

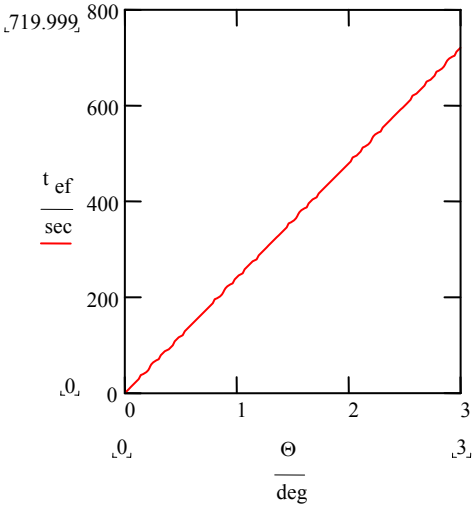

Fig. 17 POG Effective integration time

This proves to be equivalent to the integration time of the secondary mirror with exactly same field-of-view. [6] The integration time is graphed in Figure 17 for a field-of-view Θ up to 3°. Typically, this is on the order of 250 seconds for a 1° FoV, depending on the declination. To achieve the angular resolution of 0.36 arc seconds and integrate over the entire FoV would call for approximately 1000 slits laid out over the focal plane of the secondary mirror. Typically such multiple paths are created using fiber optics, but the use of lateral slits using an image slicer would permit acquisition of all objects across the lateral FoV. The requisite optical path is complex.

Allowing that there is a workable way to multiply the slits to cover the FoV of the primary, we can use the equivalency of the secondary mirror's integration time to the POG's as a means to calculate overall sensitivity. Given a 1 m^2 secondary mirror having a field-of-view of 1° and with the efficiency of the POG set at 10% we produced Table 1. A s/n of 10 can be achieved with stars a little fainter than magnitude 20 while s/n of 100 could be achieved with stars a two magnitudes brighter. Of course, lowering the spectral resolution will increase sensitivity. Spectra could be taken of objects as faint as magnitude 26 at a s/n of 10 and *R* = 1000.

Table 1 Throughput and sensitivity estimate.

item	value
atmospheric throughput	90%
grating efficiency	10%
secondary mirror reflectance (2 mirrors)	96%
field slicer throughput	90%
spectrograph throughput	83%
detector quantum efficiency	80%
total throughput	5.2%
observing wavelength	650 nm
spectral resolving power	100,000
POG length	100 m
secondary mirror area	1 m^2
secondary FoV	1°
effective integration time	240 sec
stellar magnitude	20

Another means of extending integration time is to take the POG off the strict east/west axis and dynamically track a band of the sky. The rotation would be one dimensional along the diffraction axis, that is, the requisite mobility would be over the short width dimension of the POG ribbon. This modification would not alter the low wind resistance feature, although the complication in the infrastructure over a passive POG is considerable. The gain from the process with a rotation of 75° off the line of latitude is an increase of approximately five times for the integration period. We discuss the calculation in a prior publication. [4]

While motion of a 100 m POG to track the sky is impossible, a plane grating POG can be segmented into Venetian blind subsections that can be rotated to track the precession of the sky. Tracking over 1° will increase integration time by 4 minutes.

5. CONCLUSION

Primary objective gratings operated at grazing exodus enjoy the advantage that incident radiation will be collected off to the side. When the POG is a transmission grating, the secondary optics can be buried below ground. The result is a flat surface at ground level that has no significant wind resistance regardless of the size of the primary objective element. Telescopes of this type are a novelty, and they present many challenges in their design and operation. However, when compared to proposals for giant mirrors, the advantages for the infrastructure are significant enough to justify a thorough examination of the concept.

ACKNOWLEDGEMENT

T. D. Ditto conducted his research as a Fellow of the NASA Institute for Advanced Concepts under USRA Research Subaward No. 07605-003-060.

REFERENCES

[1] Thomas D. Ditto, "The Dittoscope," Proc. SPIE 4840, *Future Giant Telescopes*, 586-597 (2003)

[2] Thomas D. Ditto, "Kilometer scale primary objective telescope with no moving parts," Proc. SPIE 4837, *Large Ground-based Telescopes*, 649-658 (2003)

[3] Thomas D. Ditto, "Kilometer scale telescope collector deployable in a shuttle payload," Proc. SPIE 5578, *Photonics North… Applications in Astronomy*…, 79-90 (2004)

[4] Thomas D. Ditto; Jeffrey F. Friedman; Jeffrey T. Baker, "Kilometer scale primary collector telescopy," Proc. SPIE 5578, *Photonics North… Applications in Astronomy*…, 68-78 (2004)

[5] Ditto and Friedman, "Gossamer Membrane Telescope," AIAA 2007-1816 (2007)

[6] David Mozurkewich, "The Sensitivity of a Spectroscopic Telescope with a Diffraction Grating Primary," Seabrook Engineering , Seabrook , MD 20706-3108, Private Communication, January 8, 2007